Removal of pseudo-convergence in near-coplanar Riemann problems of ideal magnetohydrodynamics and parallel fluid simulations on shared memory processors

Andrew Kercher

George Mason University

29 September 2014

Outline

Shocks in space plasma

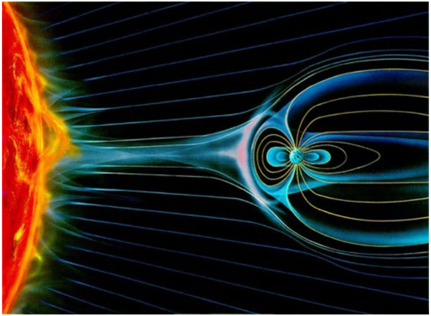

Source [10]

- Sun-earth interaction:
  - Super-sonic plasma originating at sun travels toward earth.

Shocks in space plasma

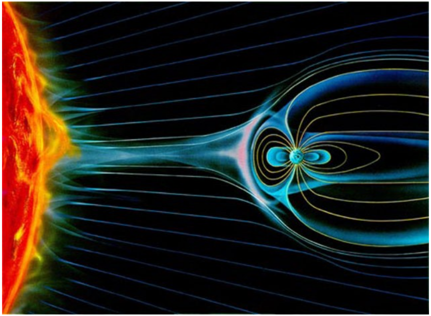

Source [10]

- Sun-earth interaction:
  - Super-sonic plasma originating at sun travels toward earth.
  - Slowed down by magnetic field of Earth.

Shocks in space plasma

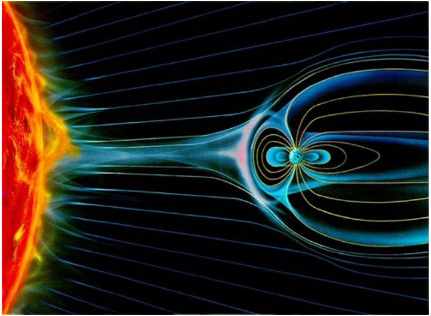

Source [10]

- Sun-earth interaction:
  - Super-sonic plasma originating at sun travels toward earth.
  - Slowed down by magnetic field of Earth.
  - Plasma flow becomes subsonic forming a bow shock.

Shocks in space plasma

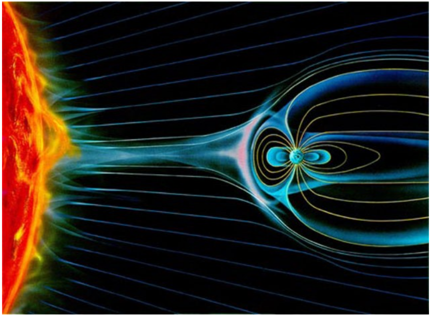

Source [10]

- 2D ideal MHD bow shock simulation. [2]
  - Results contained intermediate shocks.

Shocks in space plasma

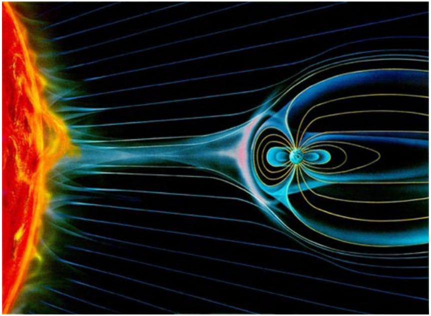

Source [10]

- 2D ideal MHD bow shock simulation. [2]
  - Results contained intermediate shocks.
  - Intermediate shocks considered inadmissible in ideal MHD [7]

Shocks in space plasma

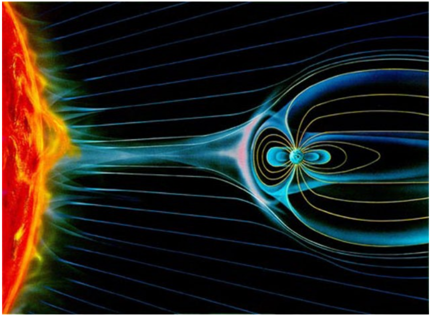

Source [10]

- 2D ideal MHD bow shock simulation. [2]
    - Results contained intermediate shocks.
    - Intermediate shocks considered inadmissible in ideal MHD [7]
    - Cause?

Overview

- Compound wave formation in MHD bow shock simulations.

Overview

- Compound wave formation in MHD bow shock simulations.
- Compound wave product of numerical diffusion.

Overview

- Compound wave formation in MHD bow shock simulations.
- Compound wave product of numerical diffusion.
- Slow convergence with finite volume schemes.

Overview

- Compound wave formation in MHD bow shock simulations.
- Compound wave product of numerical diffusion.
- Slow convergence with finite volume schemes.
- Compound wave modification (CWM).
    - Modification to the HLLD approximate Riemann solver of Athena [11].
    - Removes compound wave, correctly computes rotational discontinuity.
    - Converges at all grid resolutions.
    - FAST! HLLD intermediate states are already calculated.

Overview

- Compound wave formation in MHD bow shock simulations.
- Compound wave product of numerical diffusion.
- Slow convergence with finite volume schemes.
- Compound wave modification (CWM).
  - Modification to the HLLD approximate Riemann solver of Athena [11].
  - Removes compound wave, correctly computes rotational discontinuity.
  - Converges at all grid resolutions.
  - FAST! HLLD intermediate states are already calculated.
- Description multi-dimensional fluid solver capable of shared memory parallelism.
  - Hydrodynamics and ideal MHD.
  - Algorithms implemented for unstructured grids.

Limiting numerical diffusion

- **Total variation diminishing** (TVD): Limit slope [5].

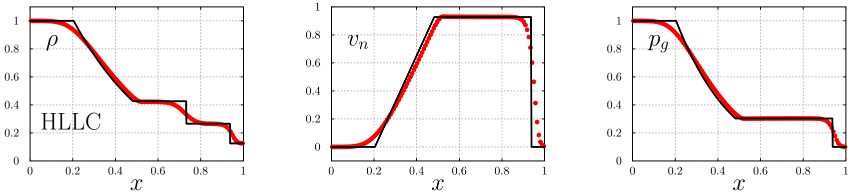

- **Flux corrected transport** (FCT): Limit flux [1].

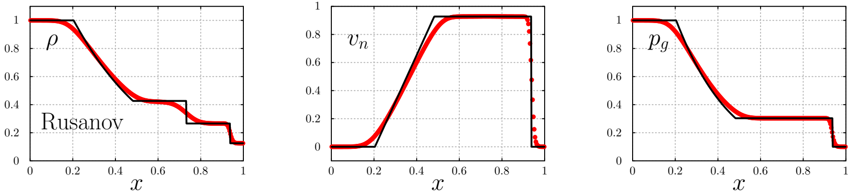

* TVD approximation computed with Athena [11].

Limiting numerical diffusion

- **Total variation diminishing** (TVD): Limit slope [5].

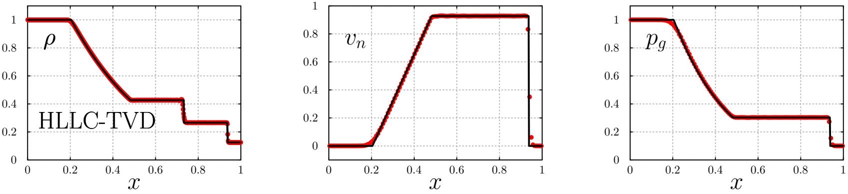

- **Flux corrected transport** (FCT): Limit flux [1].

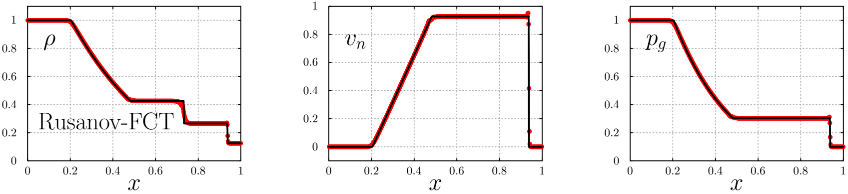

* TVD approximation computed with Athena [11].

Outline

Ideal magnetohydrodynamics

$$\frac{\partial \rho}{\partial t} + \nabla \cdot (\rho \mathbf{v}) = 0 \ ,$$

$$\frac{\partial (\rho \mathbf{v})}{\partial t} + \nabla \cdot \left[\rho \mathbf{v} \otimes \mathbf{v} + \left(p_g + \frac{B^2}{2}\right) \underline{\mathbf{I}} - \mathbf{B} \otimes \mathbf{B}\right] = 0 \ ,$$

$$\frac{\partial E}{\partial t} + \nabla \cdot \left[\left(E + p_g + \frac{B^2}{2}\right) \mathbf{v} - \mathbf{v} \cdot \mathbf{B} \otimes \mathbf{B}\right] = 0 \ , \text{ and}$$

$$\frac{\partial \mathbf{B}}{\partial t} + \nabla \cdot [\mathbf{v} \otimes \mathbf{B} - \mathbf{B} \otimes \mathbf{v}] = 0 \ ,$$

where the energy density is defined as

$$E = \frac{p_g}{\gamma - 1} + \frac{\rho v^2}{2} + \frac{B^2}{2} \ ,$$

Ideal magnetohydrodynamics

Non-strictly hyperbolic.

$$\frac{\partial \mathbf{U}}{\partial t} + \frac{\partial \mathbf{F}}{\partial x} = 0.$$

Real, but **not** necessarily distinct eigenvalues:

$$\begin{aligned}
v_n &: \text{contact or tangential discontinuity (entropy),} \\
v_n \pm c_s &: \text{slow rarefaction or shock,} \\
v_n \pm c_a &: \text{rotational discontinuity (Alfvén), and} \\
v_n \pm c_f &: \text{fast rarefaction or shock,}
\end{aligned}$$

$$c_{f,s}^2 = \frac{1}{2}\left[a^2 + c_a^2 + c_t^2 \pm \sqrt{\left(a^2 + c_a^2 + c_t^2\right)^2 - 4a^2 c_a^2}\right],$$

$$c_a^2 = \frac{B_n^2}{\rho}, \text{ and } c_t^2 = \frac{B_t^2}{\rho}.$$

Riemann problems of ideal MHD

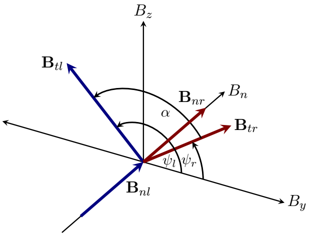

- Initial discontinuity separates two states.
- Rotation angle: $\psi = \arctan\left(B_z/B_y\right)$.
- Twist angle: $\alpha = \psi_r - \psi_l$.
- Solution: waves separating distinct states.

Riemann problems of ideal MHD

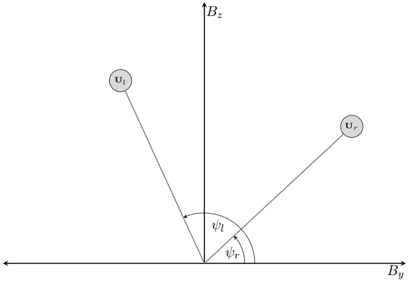

- Regular waves alter magnitude or orientation of B_t.

Riemann problems of ideal MHD

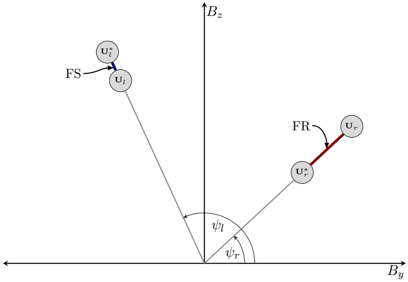

- Regular waves alter magnitude or orientation of B_t.
- Fast shock: $B_t \uparrow$, fast rarefaction: $B_t \downarrow$.

Riemann problems of ideal MHD

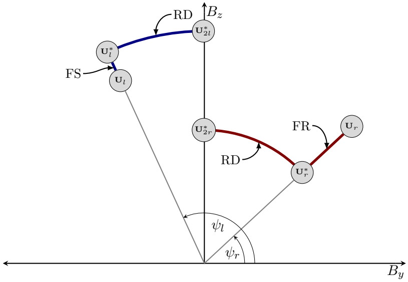

- Regular waves alter magnitude or orientation of B_t.
- Fast shock: $B_t \uparrow$, fast rarefaction: $B_t \downarrow$.
- Rotational discontinuity: $\psi \pm \delta\psi$.

Riemann problems of ideal MHD

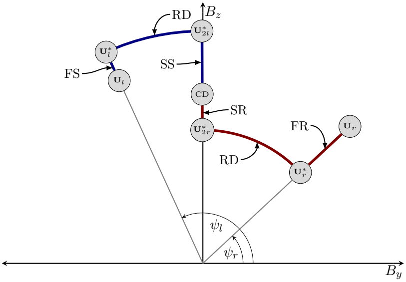

- Regular waves alter magnitude or orientation of B_t.
- Fast shock: $B_t \uparrow$, fast rarefaction: $B_t \downarrow$.
- Rotational discontinuity: $\psi \pm \delta\psi$.
- Slow shock: $B_t \downarrow$, slow rarefaction: $B_t \uparrow$.

Riemann problems of ideal MHD

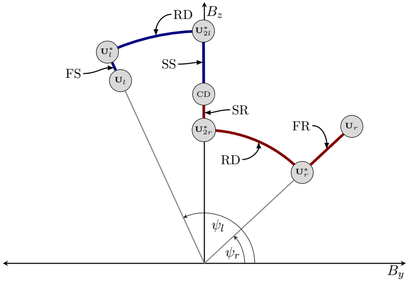

- Regular waves alter magnitude or orientation of B_t.
- Fast shock: $B_t \uparrow$, fast rarefaction: $B_t \downarrow$.
- Rotational discontinuity: $\psi \pm \delta\psi$.
- Slow shock: $B_t \downarrow$, slow rarefaction: $B_t \uparrow$.
- Contact discontinuity: no change.

Riemann problems of ideal MHD

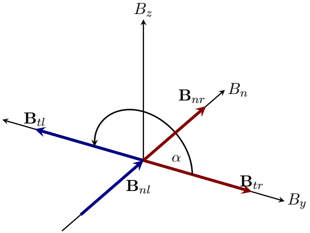

- Coplanar magnetic field

Outline

Non-unique solutions

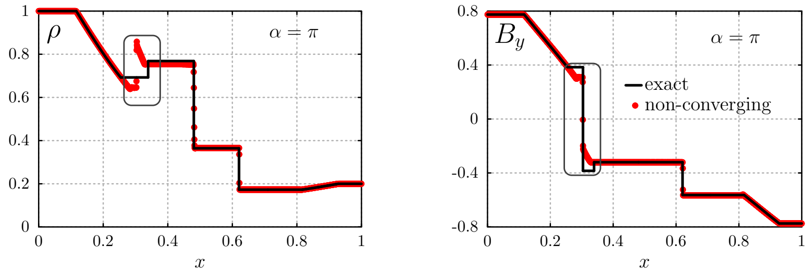

- Solutions to coplanar Riemann problems of ideal MHD are non-unique.
- At $x = 0.303$, rotational discontinuity $\to$ compound wave.

Non-unique solutions

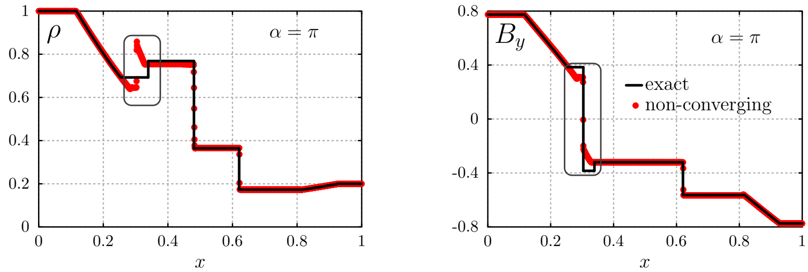

- Solutions to coplanar Riemann problems of ideal MHD are non-unique.
- At $x = 0.303$, rotational discontinuity $\rightarrow$ compound wave.
- Compound wave is composed of an intermediate shock and a slow rarefaction.
- Physical?

Non-unique solutions

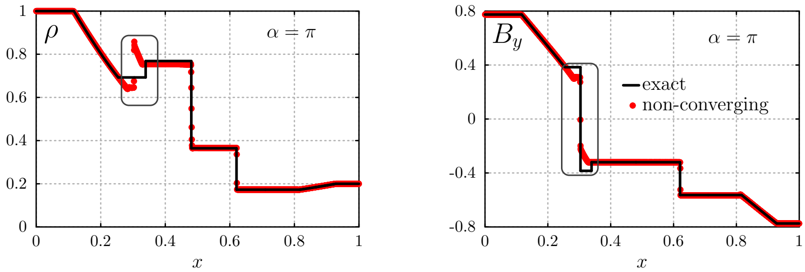

- Solutions to coplanar Riemann problems of ideal MHD are non-unique.
- At $x = 0.303$, rotational discontinuity $\rightarrow$ compound wave.
- Compound wave is composed of an intermediate shock and a slow rarefaction.
- Physical?
  - Unstable for under small perturbations [7].

Non-unique solutions

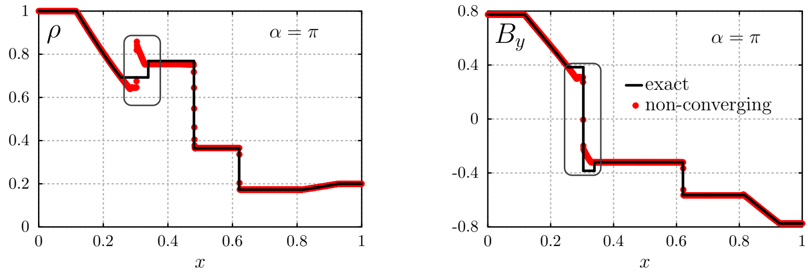

- Solutions to coplanar Riemann problems of ideal MHD are non-unique.
- At $x = 0.303$, rotational discontinuity $\rightarrow$ compound wave.
- Compound wave is composed of an intermediate shock and a slow rarefaction.
- Physical?
  - Unstable for under small perturbations [7].
  - Satisfy jump conditions (coplanar case).

Compound wave formation

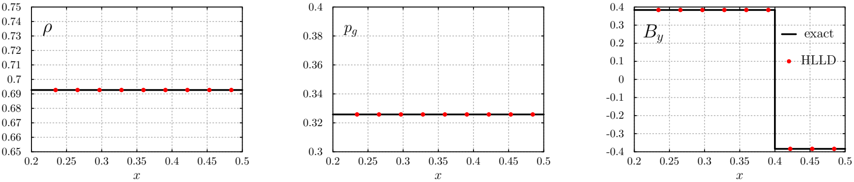

- Compound waves are a product of numerical diffusion.

Compound wave formation

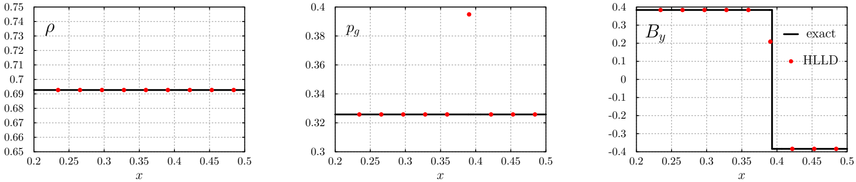

- Compound waves are a product of numerical diffusion.
- Decrease $B_t \rightarrow$ increase p_g

$$p_g = (\gamma - 1)\left(E - \frac{\rho v^2}{2} - \frac{B^2}{2}\right)$$

Compound wave formation

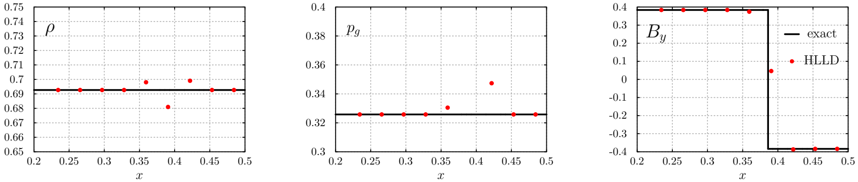

- Compound waves are a product of numerical diffusion.
- Decrease B_t $\rightarrow$ increase p_g

$$p_g = (\gamma - 1)\left(E - \frac{\rho v^2}{2} - \frac{B^2}{2}\right)$$

- Increase p_g $\rightarrow$ compound wave.

Pseudo-convergence

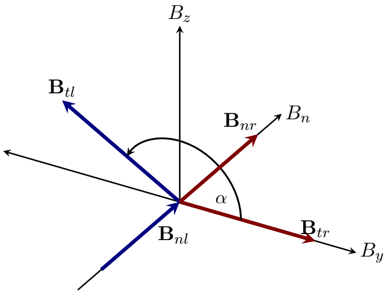

- $\alpha < \pi$, compound waves at lower resolutions.

Pseudo-convergence

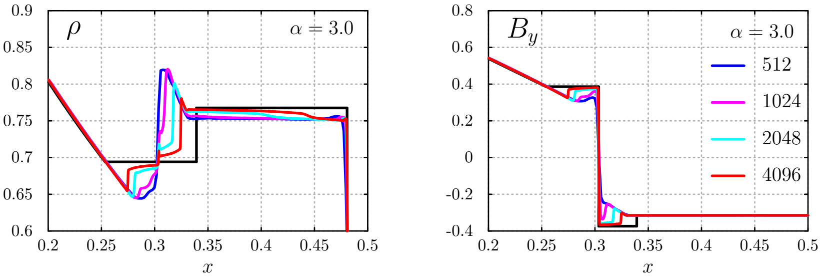

- $\alpha < \pi$, compound waves at lower resolutions.
- Pseudo-convergence: rotational discontinuity at higher resolutions [13].
- Transition between 1024 and 2048 grid points.
- $\alpha \to \pi$, grid resolution increases.
- $\pi = \alpha$, compound wave at all resolutions.

Outline

Compound wave modification

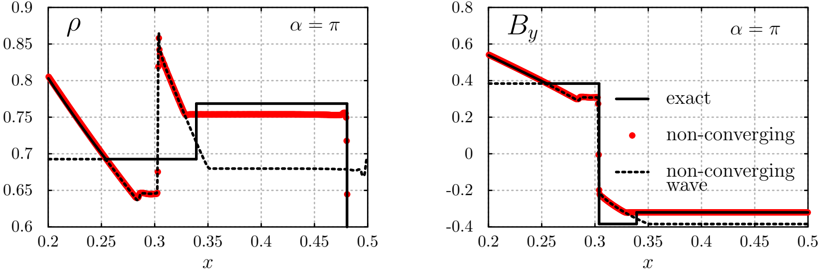

- Need to reduce numerical diffusion.

Compound wave modification

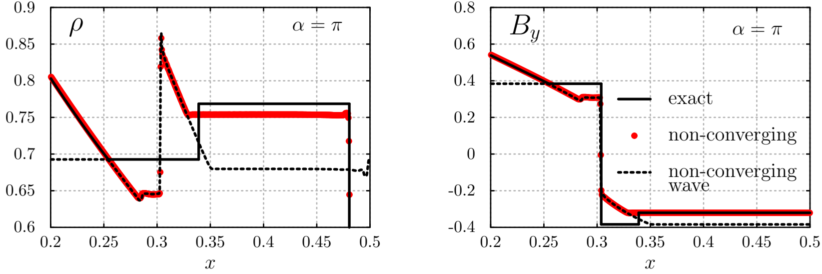

- Need to reduce numerical diffusion.
- ρ and B_t should remain constant across the rotational discontinuity $x = 0.303$.

Compound wave modification

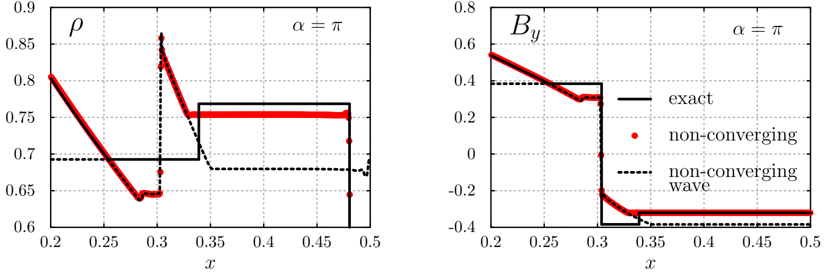

- Need to reduce numerical diffusion.
- ρ and B_t should remain constant across the rotational discontinuity $x = 0.303$.
- Limit flux associated with the compound wave.

Compound Wave modification

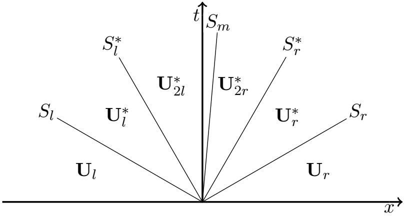

- Use HLLD to approximate intermediate states upstream and downstream of rotational discontinuity, i.e., $\mathbf{U}_\mathbf{l}^*$ and $\mathbf{U}_{2l}^*$.

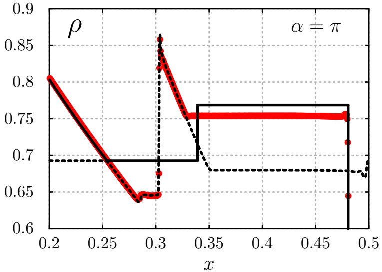

Compound Wave modification

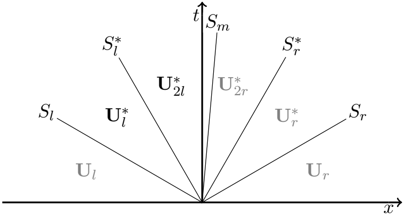

- Use HLLD to approximate intermediate states upstream and downstream of rotational discontinuity, i.e., $\mathbf{U}_\mathbf{l}^*$ and $\mathbf{U}_{2l}^*$.
- Calculate flux $\mathbf{F}^c$ between $\mathbf{U}_\mathbf{l}^*$ and $\mathbf{U}_{2l}^*$.

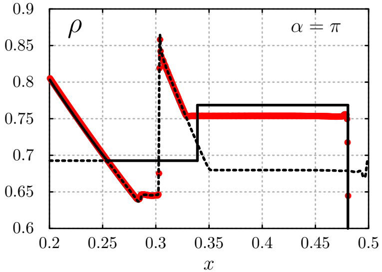

Compound Wave modification

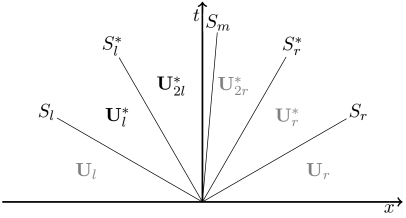

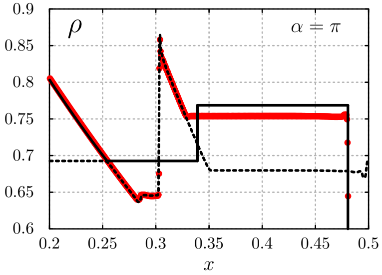

- Use HLLD to approximate intermediate states upstream and downstream of rotational discontinuity, i.e., $\mathbf{U}_\mathbf{l}^*$ and $\mathbf{U}_{2l}^*$.
- Calculate flux $\mathbf{F}^c$ between $\mathbf{U}_\mathbf{l}^*$ and $\mathbf{U}_{2l}^*$.
- Reduce the contribution of $\mathbf{F}^c = \mathbf{F}_{hlld}(\mathbf{U}_l^*, \mathbf{U}_{l2}^*)$ to the total flux.

Compound Wave modification

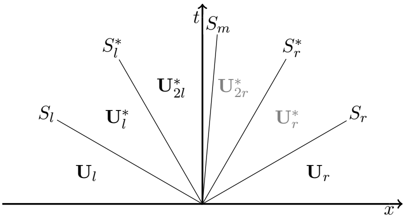

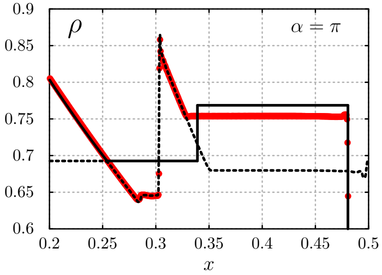

- Use HLLD to approximate intermediate states upstream and downstream of rotational discontinuity, i.e., $\mathbf{U_l^*}$ and $\mathbf{U}_{2l}^*$.
- Calculate flux $\mathbf{F}^c$ between $\mathbf{U_l^*}$ and $\mathbf{U}_{2l}^*$.
- Reduce the contribution of $\mathbf{F}^c = \mathbf{F}_{hlld}(\mathbf{U}_l^*, \mathbf{U}_{l2}^*)$ to the total flux.
- $\mathbf{F}_{cwm} = \mathbf{F}_{hlld}(\mathbf{U}_l, \mathbf{U}_r) - A\mathbf{F}^c$, where $A < 0.5$.

CWM solution

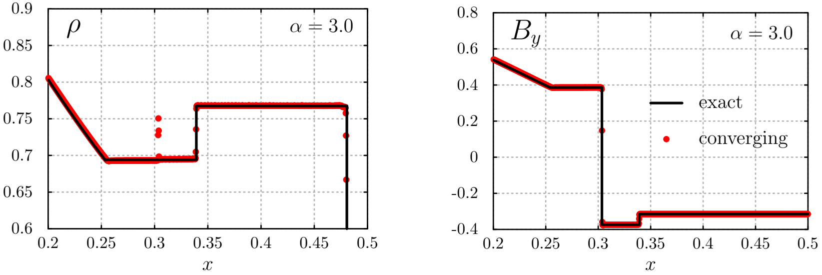

- CWM recovers the correct solution upstream and downstream of rotational discontinuity.
- Transition across rotational discontinuity is unresolved.
- Resolve it?

CWM solution

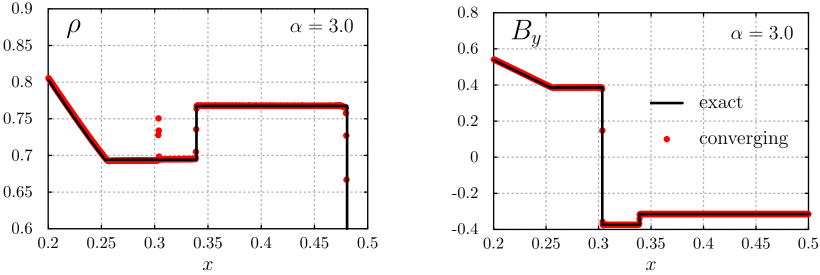

- CWM recovers the correct solution upstream and downstream of rotational discontinuity.
- Transition across rotational discontinuity is unresolved.
- Resolve it?
- Simple but non-conservative.

CWM Resolving the transition

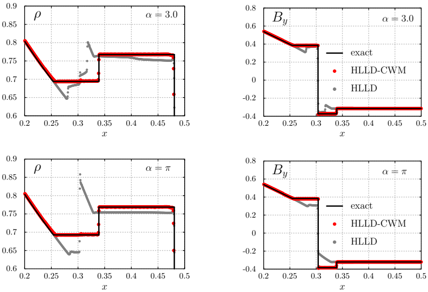

- Jump conditions in Lagrangian mass coordinates, $V = 1/\rho$, W is wave speed.
- Brackets denote difference across discontinuity.

$$
\begin{aligned}
W[V] &= -[v_n], \\
W[v_n] &= -[P - B_n^2], \\
W[\mathbf{v}_t] &= -B_n[\mathbf{B}_t], \\
W[V\mathbf{B}_t] &= -B_n[\mathbf{v}_t],
\end{aligned}
$$

CWM Resolving the transition

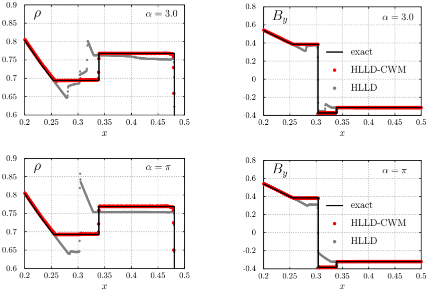

- Across rotational discontinuity

$$
\begin{aligned}
[V] &= 0, \\
[v_n] &= 0, \\
[p_g] &= 0, \\
[B_t] &= 0, \\
W[\mathbf{v}_t] &= -B_n[\mathbf{B}_t],
\end{aligned}
$$

- $W = \sqrt{\rho} B_n$ is Lagrangian speed of linear wave.

Examples

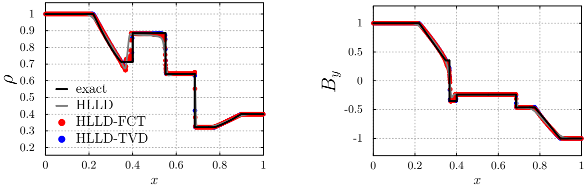

- Near coplanar initial conditions.
- Fast compound wave at $x = 0.365$

Examples

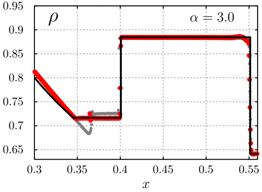

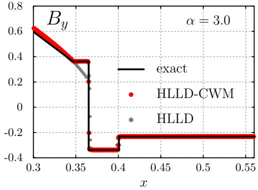

- Near coplanar initial conditions.
- Fast compound wave at $x = 0.365$
- Small deviation for weak intermediate shocks.

Examples

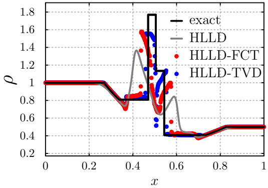

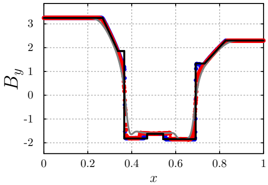

- Non-planar initial conditions.
- Fast compound waves at $x = 0.366$ and $x = 0.691$

Examples

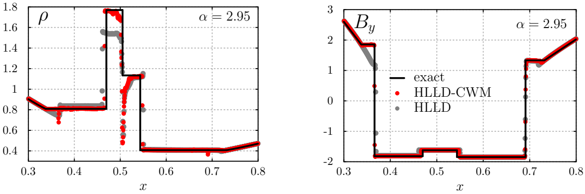

- Non-planar initial conditions.
- Fast compound waves at $x = 0.366$ and $x = 0.691$
- Small deviation for weak intermediate shocks.

Examples

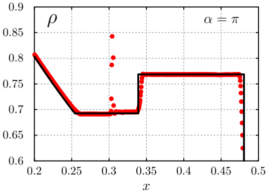

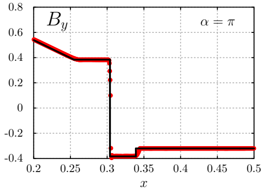

- Works with FCT!
- At rotation, set antidiffusion = CWM.
- Larger Cour. No. without additional diffusion downstream.
- Slow shock downstream poorly resolved, but weak.

Outline

Error analysis

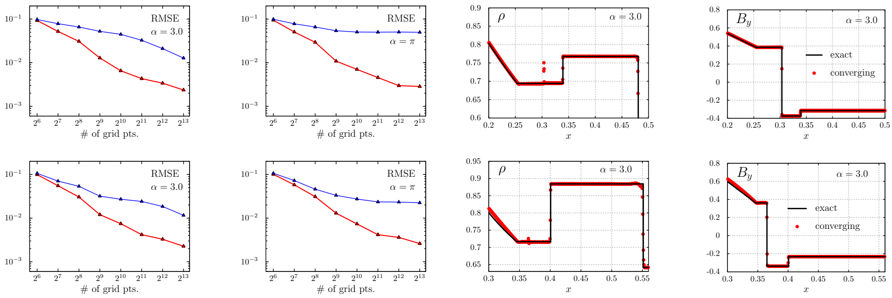

- Error calculation without applying the correction at the rotational discontinuity.
- Without CWM, the compound wave starts to break apart between 2^{10} and 2^{11}.
- CWM produces convergence at low grid resolutions.
- $\approx$ 10 times faster than exact Riemann solver.

Outline

Higher dimensions

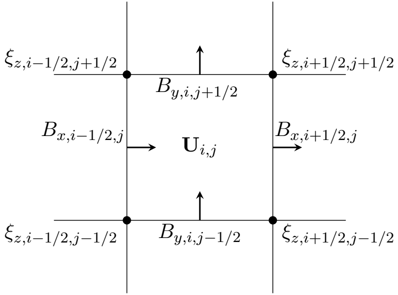

Maintaining $\nabla \cdot \mathbf{B} = 0$ with constrained transport [4].

- Staggered grid.
- Hydrodynamical variables at cell centers.
- Magnetic field at interface.
- $\mathbf{E} = -\mathbf{v} \times \mathbf{B}$ at corners.
- Denote z-component of the emf as ξ_z.

Finite area integration of interface **B**

$$B^{n+1}_{x,i+1/2,j} = B^{n}_{x,i+1/2,j} - \frac{\delta t}{\delta y}\left(\xi_{z,i+1/2,j+1/2} - \xi_{z,i+1/2,j-1/2}\right)$$

$$B^{n+1}_{y,i,j+1/2} = B^{n}_{y,i,j+1/2} + \frac{\delta t}{\delta x}\left(\xi_{z,i+1/2,j+1/2} - \xi_{z,i-1/2,j-1/2}\right)$$

Higher dimensions

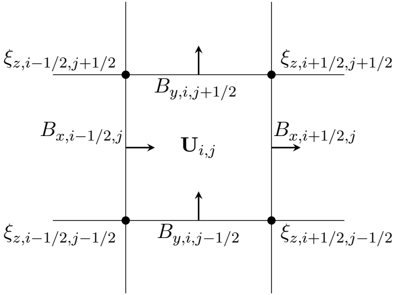

Maintaining $\nabla \cdot \mathbf{B} = 0$ with constrained transport [4].

- Staggered grid.
- Hydrodynamical variables at cell centers.
- Magnetic field at interface.
- $\mathbf{E} = -\mathbf{v} \times \mathbf{B}$ at corners.
- Denote z-component of the emf as ξ_z.

Due to perfect cancellation, the numerical divergence in the cell remains zero to machine precision.

$$(\nabla \cdot \mathbf{B})_{i,j} = \frac{1}{\delta x}\left(B_{x,i+1/2,j} - B_{x,i-1/2,j}\right) + \frac{1}{\delta y}\left(B_{y,i,j+1/2} - B_{y,i,j-1/2}\right)$$

Performance Comparison

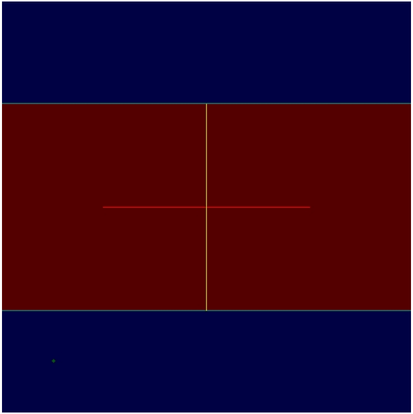

Performance comparison for Kelvin-Helmholtz Instability.

grid size	GPU/CPU
64×64	5
128×128	19
256×256	58
512×512	75
1024×1024	81

- GPU GeFroce GTX TITAN and CPU Intel Xeon E5645 @ 2.40 Ghz.
- Factor of three increase of speed ratio form 128×128 to 256×256.

Performance Comparison

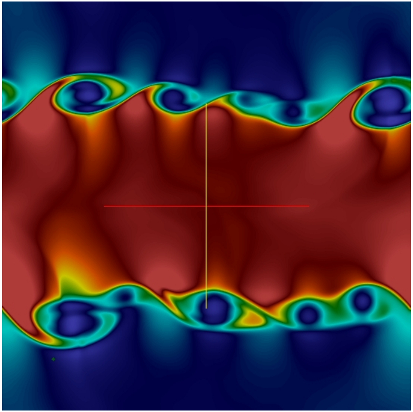

Performance comparison for Kelvin-Helmholtz Instability.

grid size	GPU/CPU
64×64	5
128×128	19
256×256	58
512×512	75
1024×1024	81

- GPU GeFroce GTX TITAN and CPU Intel Xeon E5645 @ 2.40 Ghz.
- Factor of three increase of speed ratio form 128×128 to 256×256.

Conclusion

- Compound wave modification:
  - Produces rotational discontinuity for coplanar problems.
  - Removes pseudo-convergence for near coplanar problems.
  - Does not require exact solver.
  - FAST! HLLD intermediate states are already calculated.
  - Produces the correct result when other numerical inaccuracies are present.
- Released a nonlinear solver for ideal MHD.
- Released a high-order multi-dimensional fluid solver.
  - General geometry on unstructured grids.
  - Capable of shared memory parallelism on GPU and CPU.
  - Can be used as blueprint or benchmark by anyone in computational physics and space weather communities wishing to increase performance.

Bibliography I

[1] J. P. Boris and D. L. Book. “Flux-Corrected Transport I. SHASTA, A Fluid Transport Algorithm That Works”. In: *J. Comp. Phys.* 11 (1973), pp. 38–69.

[2] H. de Sterck, B. C. Low, and S. Poedts. “Complex magnetohydrodynamic bow shock topology in field-aligned low-β flow around a perfectly conducting cylinder”. In: *Physics of Plasmas* 5 (Nov. 1998), pp. 4015–4027.

[3] B. Einfeldt. “On Godunov-Type Methods for Gas Dynamics”. In: *SIAM J. Numer. Anal.* 25 (1988), pp. 294–318.

[4] C. R. Evans and J. F. Hawley. “Simulation of magnetohydrodynamic flows - A constrained transport method”. In: *ApJ* 332 (Sept. 1988), pp. 659–677.

Bibliography II

[5] A. Harten. "High resolution schemes for hyperbolic conservation laws". In: *J. Comp. Phys.* 49 (1983), pp. 357–393.

[6] Jared Hoberock and Nathan Bell. *Thrust: A Parallel Template Library*. Version 1.7.0. 2010. URL: `http://thrust.github.io/`.

[7] L. D. Landau, E. M. Lifshitz, and L. P. Pitaevskii. *Electrodynamics of continuous media*. 3rd. 1984.

[8] T. Miyoshi and K. Kusano. "A multi-state HLL approximate Riemann solver for ideal MHD". In: *J. Comp. Phys.* 208 (May 2005), pp. 315–344.

[9] S. A. Orszag and C.-M. Tang. "Small-scale structure of two-dimensional magnetohydrodynamic turbulence". In: *Journal of Fluid Mechanics* 90 (Jan. 1979), pp. 129–143.

Bibliography III

[10] *Spasce Weather*. `http://now.uiowa.edu/files/now.uiowa.edu/styles/prim_horizontal_640/public/sun-earth-640.jpg?itok=ESKVX0GJ`.

[11] J. Stone, T. Gardner, and P. Teuben. *Athena MHD Code Project*. `https://trac.princeton.edu/Athena/`. Dec. 2010.

[12] E. F. Toro, M. Spruce, and W. Speares. "Restoration of the contact surface in the HLL-Riemann solver". In: *Shock Waves* 4 (Mar. 1994), pp. 25–34.

[13] M. Torrilhon. "Non-uniform convergence of finite volume schemes for Riemann problems of ideal magnetohydrodynamics". In: *J. Comp. Phys.* 192 (Nov. 2003), pp. 73–94.